Full Length Article

QCT of the femur: Comparison between QCTPro CTXA and MIAF Femur

Ling Wang[a,b], Oleg Museyko[b], Yongbin Su[a], Keenan Brown[c], Ruopei Yang[a], Yong Zhang[a], Yangyang Duanmu[d], Zhe Guo[a], Wei Zhang[a], Dong Yan[a], Xiaoguang Cheng[a,*], Klaus Engelke[b,e,**]

[a] Department of Radiology, Beijing Jishuitan Hospital, Beijing, China
[b] Institute of Medical Physics, University of Erlangen, Erlangen, Germany
[c] Mindways Software, Austin, TX, USA
[d] Department of Radiology, Anhui Provincial Hospital, Anhui, China
[e] Dept of Medicine 3, University Hospital Erlangen, Germany

ARTICLE INFO

ABSTRACT

QCT is commonly employed in research studies and clinical trials to measure BMD at the proximal femur. In this study we compared two analysis software options, QCTPro CTXA and MIAF-Femur, using CT scans of the semi-anthropometric European Proximal Femur Phantom (EPFP) and in vivo data from 130 Chinese elderly men and women aged 60–80 years.

Integral (Int), cortical (Cort) and trabecular (Trab) vBMD, volume, and BMC of the neck (FN), trochanter (TR), inter-trochanter (IT), and total hip (TH) VOIs were compared. Accuracy was determined in the 5 mm wide central portion of the femoral neck of the EPFP. Nominal values were: cross-sectional area (CSA) $4.9\,cm^2$, cortical thickness (C.Th) 2 mm, CortBMD $723\,mg/cm^3$ and TrabBMD $100\,mg/cm^3$. In MIAF the so-called peeled trabecular VOI was analyzed, which excludes subcortical bone to avoid partial volume artefacts at the endocortical border that artificially increase TrabBMD. For CTXA uncorrected, so called raw cortical values were used for the analysis. QCTPro and MIAF phantom results were: CSA $5.9\,cm^2$ versus $5.1\,cm^2$; C.Th 1.68 mm versus 1.92 mm; CortBMD $578\,mg/cm^3$ versus $569\,mg/cm^3$; and TrabBMD $154\,mg/cm^3$ versus $104\,mg/cm^3$.

In vivo correlations (R^2) of integral and trabecular bone parameters ranged from 0.63 to 0.96. Bland–Altman analysis for TH and FN TrabBMD showed that lower mean values were associated with higher differences, which means that TrabBMD differences between MIAF and CTXA are larger for osteoporotic than for normal patients, which can be largely explained by the inclusion of subcortical BMD in the trabecular VOI analyzed by CTXA in combination with fixed thresholds used to separate cortical from trabecular bone compartments. Correlations between CTXA corrected CortBMD and MIAF were negative, whereas raw data correlated positively with MIAF measurements for all VOIs questioning the validity of the CTXA corrections. The EPFP results demonstrated higher MIAF accuracy of cortical thickness and TrabBMD. Integral and trabecular bone parameters were highly correlated between CTXA and MIAF. Partial volume artefacts at the endocortical border artificially increased trabecular BMD by CTXA, especially for osteoporosis patients. With respect to volumetric cortical measurements with CTXA, the use raw data is recommended, because corrected data cause a negative correlation with MIAF CortBMD.

1. Introduction

Hip fracture is the most severe osteoporotic fracture, associated with high mortality and mobility. Areal bone mineral density (aBMD) determined by dual-energy X-ray absorptiometry (DXA) is an established parameter for the diagnosis of osteoporosis and the prediction of hip fracture risk. In contrast to the projectional DXA technique, quantitative computed tomography (QCT) is a 3-dimensional (3D)

technology, which provides true volumetric BMD measurements, independent of bone size. Trabecular and cortical compartments can be separated and geometrical parameters such as cortical thickness can be measured. QCT is commonly employed in research studies or clinical trials to better understand differential effects of aging and of osteoporotic interventions on cortical and trabecular bone compartments and bone strength [1,2].

The QCT analysis is typically performed outside the CT scanner on

---

workstations equipped with special software. Currently, several QCT analysis programs exist. In this study we specifically compared the commercial QCTPro (Mindways Inc., Austin, TX, USA) software frequently used by clinical sites but also in research [3–7] with the Medical Image Analysis Framework (MIAF) option Femur developed at the University of Erlangen, which has been used in most recent clinical trials in osteoporosis and a number of research studies [8–14]. Both technologies are fundamentally different. The QCTPro module for the hip called computed tomography X-ray absorptiometry (CTXA) calculates a 2D projection from the acquired 3D QCT dataset from which DXA-equivalent projectional aBMD values are derived as primary measurements. For the measurement of a true physical BMD the segmented 2D image is projected back into the 3D CT dataset.

The MIAF Femur module combines a 3D segmentation of periosteal and endosteal surfaces with the determination of anatomic coordinate systems to define volumes of interest (VOIs) for which BMD is measured. Another major difference between CTXA and MIAF-Femur is the segmentation that in particular affects cortical measurements. Technical details of CTXA and MIAF-Femur have been published before [15–17] but so far both systems have never been compared directly. It is important for potential users to recognize differences in the QCT measurements between the two systems and to understand the underlying causes. This is also a key element for standardization approaches, which are important for future use of QCT. Misunderstanding of the technology has caused misinterpretation of QCT data, cumulating for example in a invalid conclusion that QCT cannot be used to assess the cortex [18]. In this study we compared CTXA and MIAF-Femur using in vivo data from Chinese elderly men and women and a semi-anthropometric femur phantom.

2. Materials and methods

2.1. QCT-technology

2.1.1. QCTPro CTXA

CTXA is a multistep procedure. First the femoral bone is separated from surrounding soft tissue using a fixed threshold T_A with a default value of $100\,mg/cm^3$. Then the periosteal surface is further refined locally to account for cortical thickness. The adaptation is controlled by a range parameter defining the size of a local neighborhood and by a lower threshold T_B with a default value of $-250\,mg/cm^3$, although in practice the range parameter and T_B have little effect on BMD results. T_A can be modified by the user if the segmented femur contains too much soft tissue (T_A too low) or 'holes' in the trabecular compartment (T_A too high).

CTXA then calculates a 2D projectional image from the segmented femur [19]. Obviously the results depend on the direction of the projection, therefore the segmented femur must be carefully aligned manually in a predefined coordinate system. Regions of interest (ROIs) determined in the projected image are used to calculate DXA-equivalent aBMD results of the neck (FN), trochanter (TR) and intertrochanter (IT). The distal end of the IT ROI is typically adjusted to coincide with the distal end of the lesser trochanter (Fig. 1). The position of the CTXA defined FN is called fixed location neck VOI. It can be moved by the user along the neck axis, but in the analysis presented here, only the fixed location neck VOI was used. FN, TR and IT BMC and volume add up to total hip (TH) BMC and volume, respectively.

After appropriate calibration to DXA, CTXA aBMD values of the total femur and femoral neck are equivalent to DXA aBMD values and can be used to calculate T-scores according to the WHO definition of osteoporosis [17,20]. Similar to the DXA technique, CTXA often suffers from an overlap of acetabulum and femoral neck [15]. Therefore in analogy to DXA, only a narrow neck box with a width of 10 or 15 mm excluding the proximal part of the neck is analyzed and the legs should be rotated inwardly as in a DXA measurement. For subjects of small stature or with short femoral neck, rotation of the feet often does not prevent the overlap.

For the measurement of a true physical BMD in mg/cm^3 the 2D neck, trochanter and intertrochanter ROIs are projected back into the acquired 3D CT dataset to determine their 3D counterparts. This avoids a full 3D segmentation of the CT dataset. A third threshold T_C with a default value of $350\,mg/cm^3$ is used to separate cortical and trabecular bone compartments [6]. For thinner slices with a thickness of 1 mm, for example, a T_C of $450\,mg/cm^3$ is recommended. The resulting endosteal surface is not shown. Therefore the segmentation cannot be controlled and in clinical routine T_C is rarely changed.

Due to partial volume artifacts caused by the limited spatial resolution of the CT scanner, cortical volume is usually overestimated. Based on scanner specific phantom measurements, two different compensation methods have been developed for CTXA. Method A applies a correction factor that reduces cortical volume. Integral volume is reduced by the same absolute amount, trabecular volume is unaffected. Method B applies a correction factor that reduces trabecular volume. Again integral volume is reduced by the same absolute amount, but here cortical volume is unaffected. For both methods, BMC values are not corrected and corrected BMD is calculated as uncorrected BMC divided by corrected volume. The default CTXA report generated by the QCTPro software contains corrected cortical and integral BMD results using method A. Uncorrected volume and BMD values, so called 'raw' measurements, and values corrected according to method B so called 'new' measurements, can be obtained using the QCT Pro Database dump utility.

In addition to the standard CTXA analysis, QCTPro provides a bone investigational toolkit (BIT 2.0), with which an extended 2D slice based analysis along the neck axis can be performed. BIT automatically determines the slice with the minimum cross sectional area in the neck and also provides cortical thickness which is not a standard CTXA outcome. Bit uses a default T_C value of $450\,mg/cm^3$ [6]. BIT only provides raw data; it does not include a partial volume compensation method. Cortical volume is not reported on the standard BIT report but available through the QCT Pro Database dump utility. In CTXA a surrogate of cortical thickness can be estimated as cortical thickness = cortical volume / area / PI where area is the projected area of the cortical VOI as reported by CTXA.

2.1.2. MIAF-Femur

MIAF-Femur uses a very different approach of QCT image analysis. There is a direct 3D segmentation of periosteal and endosteal surfaces using local adaptive 50% thresholds combined with morphological operations [16]. Both surfaces are displayed in axial, sagittal and coronal reformation for operator control and manual editing if necessary. A wide range of 3D editing tools is available [21]. Similar to BIT, the minimum cross sectional area of the neck is determined automatically [22]. Along with the neck axis this plane is used to define a neck coordinate system, relative to which neck, trochanter, and intertrochanter VOIs are defined. In contrast to CTXA, the MIAF-Femur neck VOI includes the full neck and the distal end of the IT VOI is defined by the maximum extension of the lesser trochanter. A proximal shaft VOI and a neck box VOI can also be determined (Fig. 1). Similar to BIT, for MIAF-Femur an extended 2D analysis of slices perpendicular to the neck is available [13].

For each VOI, integral, cortical and trabecular BMD, and volume and in contrast to CTXA also cortical thicknesses are measured. BMC is calculated from BMD and volume. By default, the trabecular VOI is reduced in size by a 3D peeling to avoid partial volume artefacts at the endocortical border, that artificially increase trabecular BMD. The effect is illustrated in Fig. S1, which shows a simplified cortex as a step function and two levels of trabecular BMD representative for severe osteoporosis ($40\,mg/cm^3$) and for a healthy subject ($120\,mg/cm^3$). The Gaussian curves demonstrate the effect of partial volume artifacts due to limited spatial resolution of the CT imaging procedure. Using a threshold of 350 or $450\,mg/cm^3$ results in an overestimation of
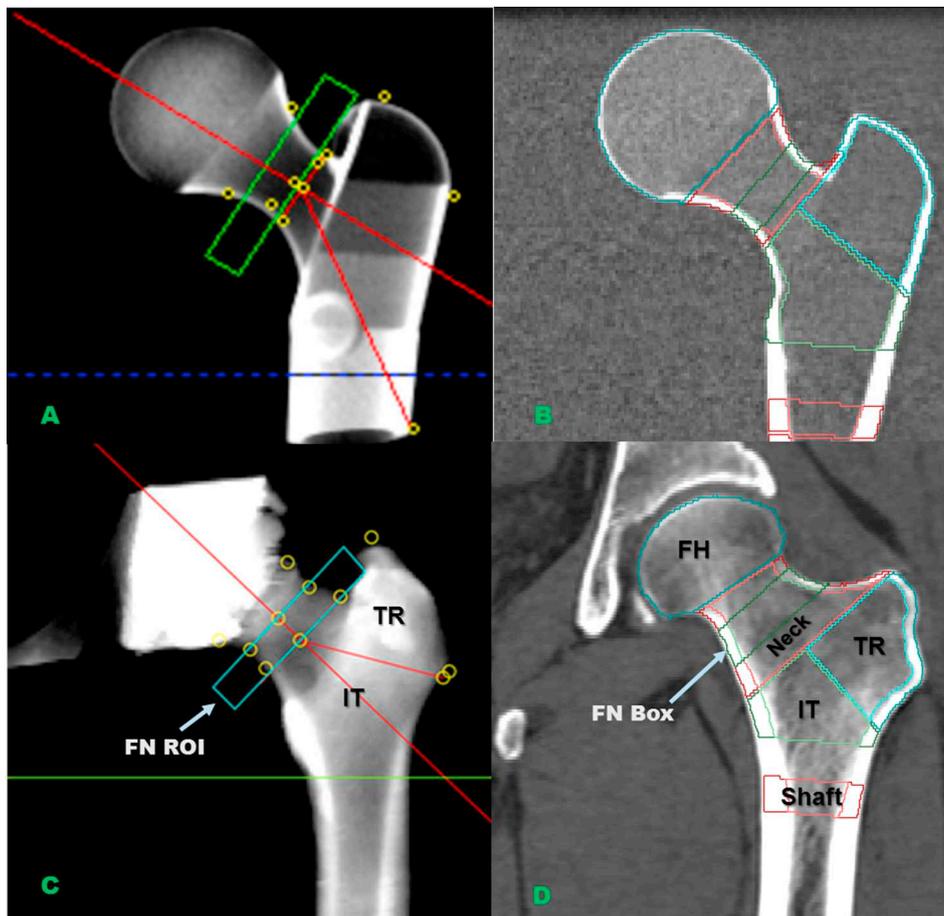
Fig. 1. Volumes of interest (VOIs) analyzed in the proximal femur by MIAF Femur and QCTPro CTXA. A & B refer to phantom image, C & D refer to VOI segmentation in vivo.

trabecular BMD that can be avoided by appropriate peeling as schematically indicated by the vertical line.

Typically in MIAF-Femur a small field of view reconstruction including one leg only, is used to benefit from slightly better spatial resolution that facilitates the segmentation process. Precision results of MIAF-Femur have been published earlier [13].

2.2. Femur phantom

The anthropomorphic European Proximal Femur phantom (EPFP; QRM GmbH, Möhrendorf, Germany) was used to compare MIAF-Femur and CTXA hip measurements. The EPFP contains a geometrically defined model of the left proximal femur with different trabecular bone mineral densities for the head, neck, trochanteric and intertrochanteric regions (Fig. 1). Nominal values of the neck VOI were: cross-sectional area (CSA) 4.9 cm^2, cortical thickness (C.Th) 2 mm, CortBMD 723 mg/cm^3 and TrabBMD 100 mg/cm^3 [23]. For the right femur, a simple cylinder of 200 mg/cm^3 HA is used. The EPFP can be used for DXA and QCT measurements of the hip.

2.3. Subjects

CT scans from 138 participants enrolled in the China Action on Spine and Hip Status (CASH) study (NTC 01758770) between March 2016 and May 2017 were included in the study. CASH is an ongoing study led by researchers at Beijing Jishuitan Hospital of Peking University, China [7]. All subjects of CASH are independently community-dwelling elderly men and women. Details of eligibility and recruitment have been previously published [6]. 8 subjects were excluded

from analysis because of a severe overlap between acetabulum and neck in the CTXA image. Thus, 130 individuals (age: 60 to 80 years, mean ± SD 70.1 ± 6.5 years) were included in the final sample size, including 61 males and 69 females. Institutional Review Board (IRB) approval was obtained from the ethics committee of Beijing Jishuitan Hospital and signed informed consent form was obtained from the participants before the scan.

2.4. QCT procedure

2.4.1. CT acquisition

The EPFP was scanned (120 kV, 200 mAs, pitch 1, 1 mm reconstructed slice thickness of 1 mm reconstruction increment, 50 cm reconstruction field of view, medium reconstruction kernel (B40s) on a 64-slice Siemens Somatom Definition CT scanner (Siemens, Erlangen, Germany) on top of a Mindways calibration phantom (Mindways Software Inc., Austin, TX, USA).

In vivo hip CT scans were acquired on an Aquilion Prime CT scanner (Toshiba Medical Systems Corp., Tokyo, Japan) extending from 1 cm above the femoral head to 3 cm below the lesser trochanter using the same acquisition parameters with exception of a lower exposure (125 mAs) and the scanner specific medium reconstruction kernel FC08. Subjects were also scanned on top of the Mindways calibration phantom as described previously [7].

2.4.2. QCT analysis

The study analysis is outlined in Fig. S2. The aim of the EPFP scans was to evaluate accuracy. The in vivo scans were used to compare integral, trabecular and cortical parameters. For all analyses CTXA

version 4.2.3 and MIAF-Femur version 6.2.0 were used.

2.4.2.1. EPFP analysis. In order to compare cortical results from the EPFP scans, for MIAF a neckbox with a width of 5 mm was analyzed. The MIAF neckbox is automatically positioned in the center of the neck of the EPFP where nominal trabecular and cortical BMD and cortical thickness are well defined. CTXA does not provide cortical thickness, therefore the BIT tool was used for cortical measurements. Results were obtained as average values from five 1 mm thick slices positioned in the center of the EPFP neck to match the MIAF neckbox as close as possible. For BIT, raw data were analyzed, only. Two different values of T_C were used: 350 and 450 mg/cm^3. For MIAF the trabecular VOI was peeled by 1.5 mm.

2.4.2.2. Subject analysis. For all patients the left hip was analyzed. In CTXA the left hip was selected using the standard procedure. T_C was set to 450 mg/cm^3 for all scans and the default neckbox, which is not positioned in the center of the neck was used. Unless noted otherwise, raw data were used for the CTXA analysis.

For MIAF, a small FOV reconstruction of the left hip was interpolated from the existing large FOV reconstruction using a Lancos windowed sync approach. Trabecular VOIs were peeled using a distance of 1.5 mm. Instead of the complete neck VOI, a femoral neckbox with a width of 10 mm was used for the comparison with CTXA results. Nevertheless, the MIAF total hip VOI was defined as sum of neck, trochanter and intertrochanteric VOIs.

2.5. Statistics

Continuous variables were described as mean ± standard deviation (SD). Both MIAF-Femur and CTXA analyses were performed by the same expert operator (L. Wang). Paired Student's *t*-tests were used to assess differences between CTXA and MIAF. The relationship between CTXA and MIAF measurements and Pearson correlation coefficients were analyzed using linear regression analysis. Bland-Altman analyses were used to describe the consistency between parameters computed by CTXA and MIAF-Femur. All statistical analyses were performed with IBM SPSS Statistics version 20.0 (IBM SPSS Inc., Chicago, IL), with $p < 0.05$ being considered statistically significant.

3. Results

3.1. EPFP phantom

Results are shown in Fig. 2. Independent of threshold T_C, BIT overestimated CSA by 20% or 1 cm^2. Overestimation by MIAF was 4%. Depending on T_C, BIT either underestimated cortical thickness by 15% or overestimated it by 12%. MIAF underestimated cortical thickness by 4%. There was comparable underestimation of cortical BMD between BIT and MIAF. Due to partial volume artifacts, BIT overestimated trabecular BMD, in particular when using the higher threshold of 450 mg/cm^3. For MIAF-Femur accuracy of trabecular BMD was excellent (Fig. 2).

3.2. Subjects

130 subjects with a mean age of 70.1 ± 6.5 years, a mean height of 163.4 ± 7.8 cm, and a mean weight of 68.1 ± 9.8 kg were included in the study. Table 1 shows comparisons of integral and trabecular BMD and volume between MIAF and CTXA. For the purpose of this analysis we will use the term neck in accordance with the CTXA analysis which in reality only uses a neckbox. MIAF neck results are also given for the neckbox. The width of the CTXA and MIAF neckbox was identical but in subjects anatomical positions differed slightly.

In Table 1 correlation coefficients (R^2) ranged from 0.63 (ITIntgVol) to 0.96 (TRIntgBMD). *p*-Values of corresponding regressions were <

0.001 for all variables shown in Table 1. Fig. 3 shows scatter plots for total hip and femoral neck and corresponding Bland–Altman (BA) plots. For all variables shown in Table 1 values differed significantly between CTXA and MIAF-Femur but it must be considered that analyses VOIs also differed. The trabecular VOI of MIAF-Femur is expected to be smaller than for CTXA because of the peeling used by MIAF-Femur. The BA plots in Fig. 3 show a negative slope in particular for trabecular BMD. At a mean total hip trabecular BMD of 150 mg/cm^3 CTXA results were about 40 mg/cm^3 higher than MIAF-Femur results. This difference almost doubled to about 70 mg/cm^3 for a mean trabecular BMD of 80 mg/cm^3. Similar results for trabecular BMD were obtained for the neck.

Table 2 shows cortical BMD, BMC and volume for MIAF and CTXA. With exception of the intertrochanter, cortical volume results were lower and cortical BMD results were higher for CTXA. Again all values shown in the table differed significantly between the two systems. Correlations were high to moderate with R^2 values above 0.6 for cortical BMC with the exception of the IT VOI but much lower for cortical volume and BMD. BA plots for total hip and neckbox cortical BMD and BMC are shown in Fig. 4. As with trabecular BMD, there was a negative slope for cortical BMD. CTXA was higher than MIAF total hip cortical BMD by 400 mg/cm^3 for lower and by 250 mg/cm^3 for higher cortical BMD values, corresponding values at neck were 350 mg/cm^3 and 200 mg/cm^3, respectively.

Finally Fig. 5 shows the correlation between MIAF and CTXA for raw and corrected cortical BMD (Method 1). It shows an expected positive regression slope for raw but a negative slope for corrected cortical BMD values. Also for CTXA the mean of the corrected BMD values were larger than 1200 mg/cm^3, which represents fully mineralized bone.

4. Discussion

In this study, two software programs frequently used for the analysis of QCT scans of the hip were compared. As indicated by its name, the main purpose of CTXA is to obtain DXA equivalent T-scores from CT scans. Areal BMD measurements from CTXA have been integrated in the FRAX tool [24] for fracture prediction. Although one would not perform a QCT procedure just to calculate DXA-equivalent T-scores, in opportunistic screening the calculation of T-scores from existing CT scans is an attractive feature. In contrast to CTXA, the major aim of MIAF-Femur is to obtain information of the proximal femur not available from DXA scans [13]. While it does not provide an option to simulate DXA equivalent data, MIAF-Femur offers a direct 3D segmentation. Periosteal and endosteal surfaces are displayed and can be corrected by the operator if necessary. In CTXA the endocortical surface is not shown and the periosteal surface cannot be edited locally.

The partial volume compensation methods developed for CTXA simply apply a numerical correction of measured cortical (method A) or trabecular volume (method B) but do not apply advanced deconvolution methods developed to more accurately segment the cortical compartment in case of thin cortices [25–28]. Both CTXA compensation methods use information regarding bone volume to projected area and are based upon estimates of in-plane (axial) image spatial resolution. With method A too much of the partial volume error is assigned to the cortical bone compartment. In extreme cases, this can result in negative cortical bone volume estimates. In less extreme cases it results in a more modest overestimation of cortical density due to the underestimation of cortical bone volume. Method B is constrained to prevent negative cortical volume estimates by better portioning the partial volume error between cortical and trabecular bone compartments.

Our results show that total hip integral volume was highly correlated between MIAF and raw data from CTXA. Differences can be explained by differences in segmentation and VOI definitions. The phantom results demonstrated that CTXA overestimated integral CSA, i.e. volume by 20%. This finding was confirmed in subjects, where a difference of 17.4% in integral volume was observed in the neckbox,

Femoral neck

	Min-CSA 4.9cm² EPFP Ref.	Min-CSA 5.1cm² MIAF		Min-CSA 5.9cm² BIT(450)		Min-CSA 5.9cm² BIT(350)

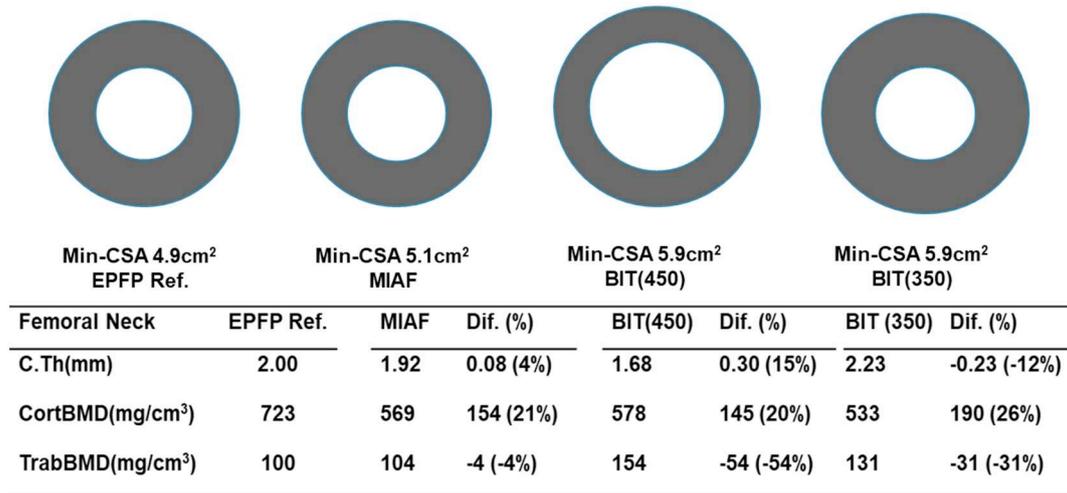| Femoral Neck	EPFP Ref.	MIAF	Dif. (%)	BIT(450)	Dif. (%)	BIT (350)	Dif. (%)
C.Th(mm)	2.00	1.92	0.08 (4%)	1.68	0.30 (15%)	2.23	-0.23 (-12%)
CortBMD(mg/cm³)	723	569	154 (21%)	578	145 (20%)	533	190 (26%)
TrabBMD(mg/cm³)	100	104	-4 (-4%)	154	-54 (-54%)	131	-31 (-31%)

Fig. 2. MIAF and QCTPro BIT results of the EPFP analysis. The pictograms show from left to right: a cross section of the EPFP at the smallest cross sectional area (Min-CSA) in the neck and the perceived cross sections from the MIAF and the QCTPro analysis. Cortical thickness (C.Th), and cortical (CortBMD) and trabecular BMD (TrabBMD) are shown as nominal values of the EPFP [23] along with the measured values obtained from the MIAF and QCTPro BIT analysis. Absolute and percentage differences (Dif) between nominal and measured values are also shown.

the VOI most comparable in size and position between MIAF and CTXA. A similar overestimation of integral volume was found the total hip indicating that differences in the definition of the intertrochanteric border and the neck VOI may largely cancel out. Comparison of integral volume of the sub VOIs is more difficult due to different definitions, which also explains the lower correlation when compared to total hip volume.

The same is true for integral BMD, although as expected correlations were higher than for integral volume because differences in volume and BMC mostly eliminate each other. The BA plot for total hip integral BMD showed no slope, there was just a mean bias of about 30 mg/cm². Correlations for integral BMD were also high for the femoral neck, trochanter and intertrochanter.

The interpretation of trabecular BMD results is more subtle. Correlations between CTXA and MIAF were almost as high as for integral BMD although due to the exclusion of subcortical bone, trabecular BMD and volume were lower for MIAF. Most important however, the BA plots showed that the difference in trabecular BMD depended on the absolute trabecular BMD. This is a direct consequence of the fixed CTXA threshold T_C in combination with the inclusion of the subcortical region. Fig. S1 shows a simple step model of cortical and trabecular

bone. The red curve simulates the effect of the limited spatial resolution of the CT scanner assuming a trabecular BMD of 120 mg/cm³ and the blue curve assuming a trabecular BMD of 40 mg/cm³. MIAF excludes but CTXA includes the subcortical compartment between points A and B in the trabecular measurement. The area under the red and blue curves between A and B were 26.4 and 29.6 mg, respectively. A and B define a total length of 4 mm, identical for both cases. This simplistic simulation nevertheless shows that with increasing trabecular BMD the contribution of the subcortical BMC and BMD to the CTXA result decreases, explaining the effect shown in the BA plots of Fig. 3. Between osteoporotic and healthy subjects the accuracy error in CTXA trabecular BMD varies by about 60 mg/cm³, which demonstrates the problem of using a fixed T_C instead of more advanced segmentation thresholds. Thus, CTXA trabecular BMD values have to be interpreted with caution.

Accuracy of cortical values was also evaluated in the EPFP scan. CTXA and MIAF, both showed an underestimation of cortical BMD by 20% to 26%. The MIAF results were accurate for CSA and cortical thickness but show that even if cortical thickness is accurate, partial volume artifacts cause a significant accuracy error in cortical BMD. Accuracy of cortical BMD will increase with thicker cortices. For thinner cortices there will be an increasing overestimation of cortical

Table 1
Integral and trabecular BMD and volume for CTXA raw data and MIAF-Femur. Differences were significant ($p < 0.05$) for all variables. TH: total hip; FN: femoral neck (for MIAF-Femur: femoral neck box); TR: trochanter; IT: intertrochanter; SEE: standard error of estimate of the linear regression.

| VOI	Variable	QCTPro (n = 130)	MIAF (n = 130)	Abs Diff (% Diff)	R^2	Slope	SEE
TH	IntgBMD (mg/cm³)	272.7 ± 43.6	240 ± 41	32.7 (12)	0.91	0.90	13.2
	TrabBMD (mg/cm³)	151.3 ± 21.7	94.3 ± 31.7	57 (37.7)	0.88	1.38	7.6
	IntgVol (cm³)	92.4 ± 18.6	75.2 ± 16.8	17.2 (18.6)	0.90	0.86	5.8
	TrabVol (cm³)	76.5 ± 16	42.9 ± 11.5	33.6 (43.9)	0.91	0.69	4.9
FN	IntgBMD (mg/cm³)	273.8 ± 47.1	287 ± 54.9	−13.2 (−4.8)	0.94	1.13	11.9
	TrabBMD (mg/cm³)	157.1 ± 27.4	108.5 ± 42.5	48.6 (30.9)	0.73	1.33	14.4
	IntgVol (cm³)	8.6 ± 1.5	7.1 ± 1.3	1.5 (17.4)	0.80	0.76	0.7
	TrabVol (cm³)	7.1 ± 1.5	3.7 ± 1	3.4 (47.9)	0.80	0.59	0.7
TR	IntgBMD (mg/cm³)	183.8 ± 33.9	199.5 ± 37.3	−15.7 (−8.5)	0.96	1.07	6.4
	TrabBMD (mg/cm³)	151.3 ± 21	79 ± 27.8	72.3 (47.8)	0.85	1.20	8.1
	IntgVol (cm³)	32.5 ± 7.8	29.2 ± 6.6	3.3 (10.2)	0.73	0.72	4.1
	TrabVol (cm³)	30.3 ± 7.2	16.2 ± 4.4	14.1 (46.5)	0.73	0.52	3.8
IT	IntgBMD (mg/cm³)	328.1 ± 54.3	256.7 ± 50.1	71.4 (21.8)	0.82	0.84	23.2
	TrabBMD (mg/cm³)	150.3 ± 24.4	96.9 ± 35.6	53.4 (35.5)	0.87	1.39	8.8
	IntgVol (cm³)	51.3 ± 10.6	26.1 ± 7.2	25.2 (49.1)	0.63	0.55	6.5
	TrabVol (cm³)	39.1 ± 8.6	16.3 ± 4.9	22.8 (58.3)	0.69	0.48	4.8
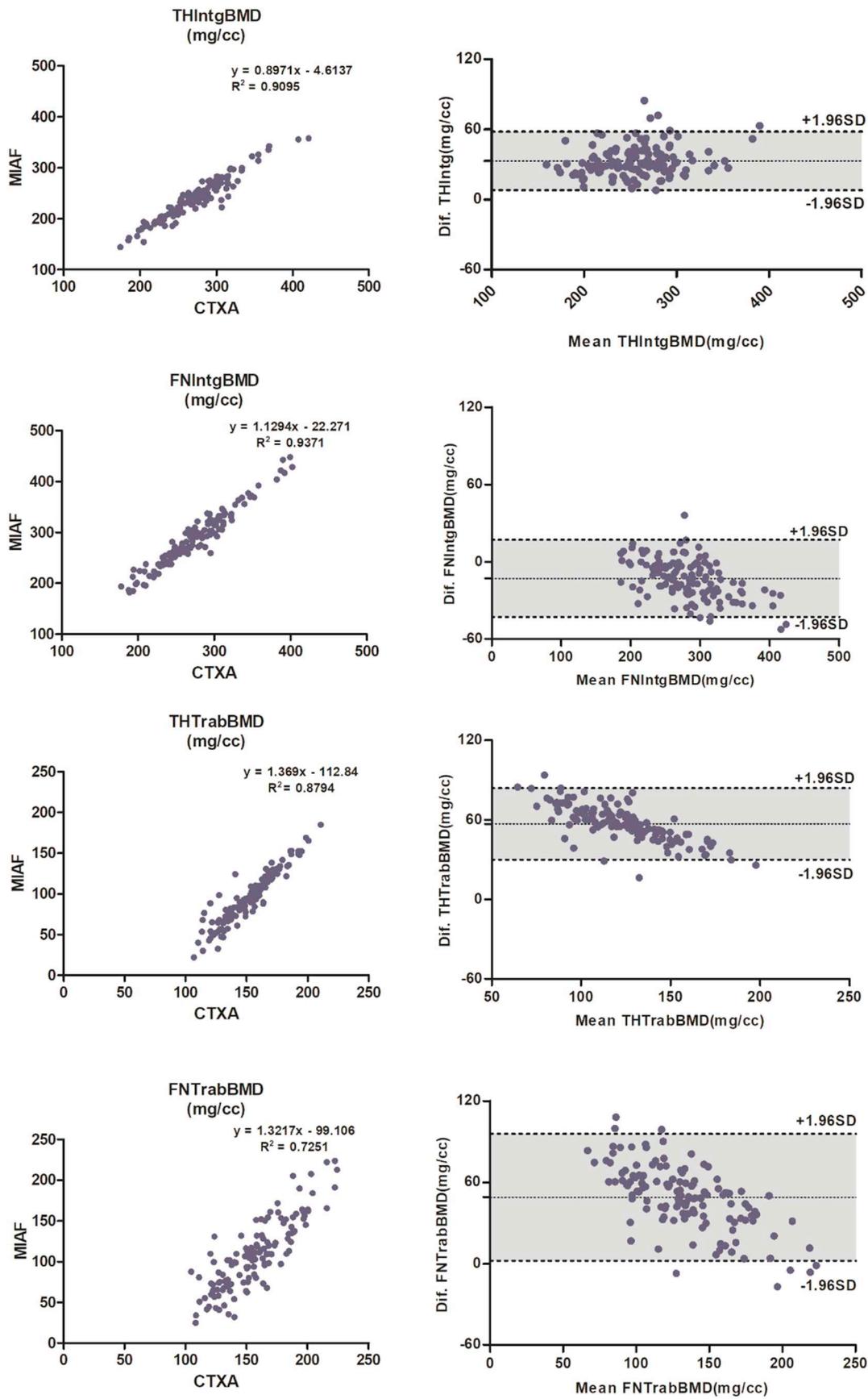
Fig. 3. Plots and Bland-Altman analysis of MIAF and CTXA measurements for integral and trabecular bone of total hip (TH) and femoral neck (FN).

Table 2
Comparisons of cortical bone parameters between QCTPro and MIAF Femur in vivo.

| VOI	Variable	QCTPro (n = 130)	MIAF (n = 130)	Abs Diff (% Diff)	R^2	Slope	SEE
TH	CortBMD (mg/cm^3)	855 ± 37	530 ± 63	324.6 (38)	0.11	0.56	35.0
	CortVol (cm^3)	15.9 ± 4.8	21.2 ± 3.9	−5.3 (−33.3)	0.36	0.49	3.8
	CortBMC (mg)	13,645 ± 4224	11,313 ± 2680	2332 (17.1)	0.63	0.50	2569
FN	CortBMD (mg/cm^3)	833 ± 49	573 ± 73	259.6 (31.2)	0.004	0.099	48.9
	CortVol (cm^3)	1.5 ± 0.4	2.3 ± 0.3	−0.8 (−53.3)	0.11	0.23	0.4
	CortBMC (mg)	1221 ± 351	1304 ± 226	−83.5 (−6.8)	0.62	0.51	216
TR	CortBMD (mg/cm^3)	633 ± 31	426 ± 67	206.4 (32.6)	0.48	1.49	22.5
	CortVol (cm^3)	2.2 ± 1.4	8.4 ± 1.6	−6.2 (−281.8)	0.13	0.41	1.3
	CortBMC (mg)	1432 ± 939	3597 ± 915	−2166 (−151.3)	0.61	0.77	588
IT	CortBMD (mg/cm^3)	894 ± 44	647 ± 75	247.1 (27.6)	0.32	0.96	36.7
	CortVol (cm^3)	12.2 ± 3.4	6.5 ± 1.7	5.7 (46.7)	0.31	0.28	2.9
	CortBMC (mg)	10,993 ± 3355	4225 ± 1365	6768 (61.6)	0.39	0.25	2627
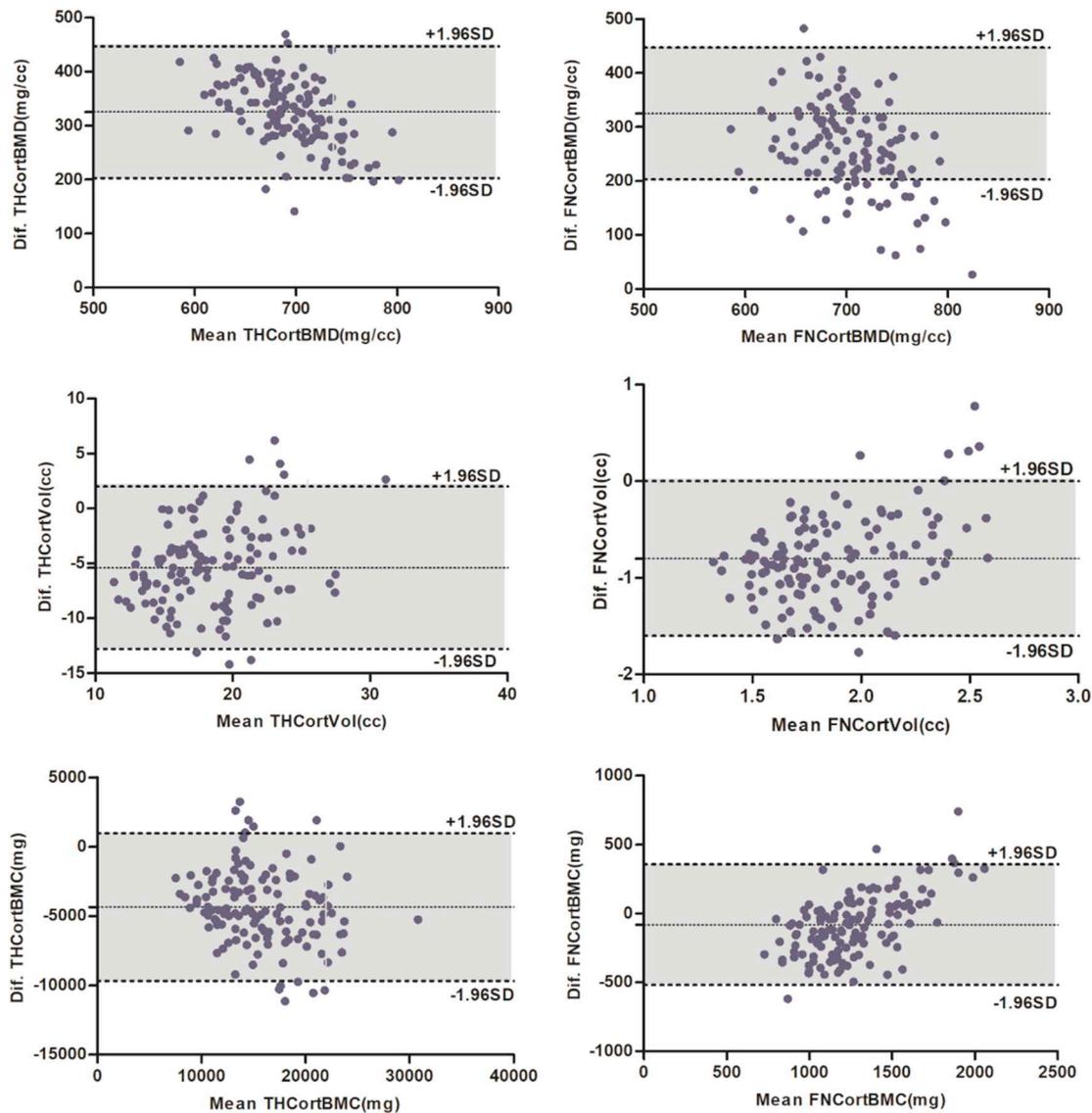
Fig. 4. Bland-Altman plots of raw CTXA and MIAF measurements for cortical bone.

thickness unless deconvolution based segmentation methods are used [25–28]. The EPFP results also demonstrate the dependence of cortical BMD and cortical thickness on T_C using values of 450 to 350 mg/cm^3. Unfortunately there is no standard for selecting the value of T_C. Although 350 mg/cm^3 or 450 mg/cm^3 are preferred values for the analysis of subject data [6,29–32] some studies used 250 mg/cm^3, 300 mg/cm^3 or 400 mg/cm^3 for specific VOIs [3,33,34]. In our subject analysis a

T_C of 450 mg/cm^3 was used.

In vivo correlations between CTXA and MIAF were poor for cortical BMD values but moderate for cortical BMC (Table 2). Absolute BMC values differed by only 7% in the neckbox, the VOI most comparable between CTXA and MIAF. Due to differences in size, absolute values are difficult to compare for the other VOIs. Another complication is the missing visualization of the CTXA segmentation. In MIAF cortical
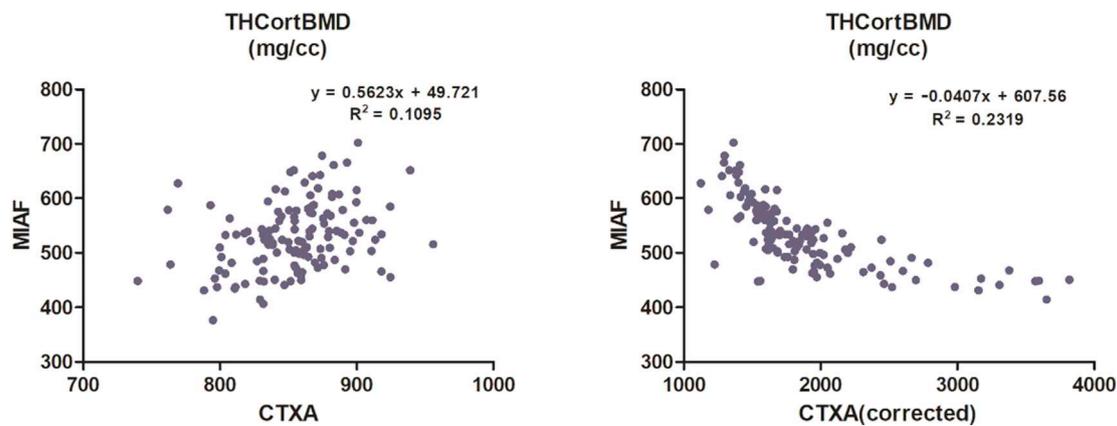
THCortBMD (mg/cc)

$$y = 0.5623x + 49.721$$
$$R^2 = 0.1095$$

THCortBMD (mg/cc)

$$y = -0.0407x + 607.56$$
$$R^2 = 0.2319$$

Fig. 5. Inconsistency in total hip (TH) cortical vBMD caused by adjustments applied by CTXA. Left: CTXA raw data. Right: CTXA data corrected with method A.

volume is overestimated, in particular in the neck VOI, but visual inspections confirmed that the cortex was fully included in the cortical VOI. Despite moderate correlations, the BA plots in Fig. 4 show a large slope for cortical BMC, again pointing out limitations of the use of global thresholds in CTXA. Finally Fig. 5 confirms earlier reports that corrected cortical values, which are shown on the CTXA reports should not be used and may lead to erroneous conclusions about the value of QCT [1,18]. Interpretation of corrected cortical results used in earlier studies should perhaps be revisited. However, most studies using CTXA focused on areal BMD or applied BIT which only uses uncorrected cortical data and conclusions of these studies will not be affected.

There are several limitations in our study. First, by default MIAF-Femur uses a dataset reconstructed with a small FOV of 150 mm for analysis, but for the CT datasets used in this study only a large FOV reconstruction was available. Thus all datasets were resampled using interpolation. Different definitions of the VOIs somewhat limited the comparability and the missing visualization of the cortical VOI in CTXA severely limited the comparison of the cortical results. Differences in particular in cortical and trabecular BMD and volume indicate an urgent need for standardization. Currently it is not even possible to export segmentation masks from or import them into CTXA, a potential first step towards standardization.

In conclusion, the primary use of CTXA should be limited to the analysis of aBMD, which provides DXA equivalent hip T-scores. This is a very important for opportunistic screening using existing CT data. The use of CTXA for a volumetric analysis of BMD is more problematic. Integral values of the total hip agree well with the MIAF analysis but trabecular and cortical values strongly depend on the selected thresholds. A major problem of CTXA is the missing visualization of the endosteal border preventing any user based corrections of potential exclusion of data in case of segmentation failure. The segmentation of the 2D projections requires a tight control of leg rotation during the CT acquisition but overlap of acetabulum and femoral neck still cannot be completely avoided in CTXA. This problem does not exist if a true 3D segmentation is applied directly to the CT data. The use of CTXA corrected cortical data is strongly discouraged. The study results further underscore the need of standardization of analysis VOIS and cortical segmentation algorithms.

Authorship

All authors made substantial contributions to all of the following: (1) the conception and design of the study, or acquisition of data, or analysis and interpretation of data, (2) drafting the article or revising it critically for important intellectual content, (3) final approval of the version to be submitted.

Conflicts of interest

Klaus Engelke is a part time employee of BioClinica, Inc. Keenan Brown is a stockholder of Mindways Software Inc.

Appendix A. Supplementary data

Supplementary data to this article can be found online at https://doi.org/10.1016/j.bone.2018.10.016.

References

[1] K. Engelke, Quantitative computed tomography-current status and new developments, J. Clin. Densitom. 20 (3) (2017) 309–321.

[2] K. Engelke, B.v. Rietbergen, P. Zysset, FEA to Measure Bone Strength: A Review, Clin. Rev. Bone Miner. Metab. 14 (2016) 26–37.

[3] J. Borggrefe, et al., Quantitative computed tomographic assessment of the effects of 24 months of teriparatide treatment on 3D femoral neck bone distribution, geometry, and bone strength: results from the EUROFORS study, J. Bone Miner. Res. 25 (3) (2010) 472–481.

[4] M. Ito, et al., Analysis of hip geometry by clinical CT for the assessment of hip fracture risk in elderly Japanese women, Bone 46 (2) (2010) 453–457.

[5] Y. Luo, H. Yang, Comparison of femur stiffness measured from DXA and QCT for assessment of hip fracture risk, J. Bone Miner. Metab. (2018), https://doi.org/10.1007/s00774-018-0926-z [Epub ahead of print].

[6] L. Wang, et al., Sex-related variations in cortical and trabecular bone of the femoral neck in an elderly Chinese population, Osteoporos. Int. 28 (8) (2017) 2391–2399.

[7] L. Wang, et al., Differences in femoral neck structure between elderly Caucasian and Chinese populations: a cross-sectional study of Perth-Beijing cohorts, Arch. Osteoporos. 12 (1) (2017) 72.

[8] V.D. Bousson, et al., In vivo discrimination of hip fracture with quantitative computed tomography: results from the prospective European Femur Fracture Study (EFFECT), JBMR 26 (4) (2011) 881–893.

[9] K. Engelke, et al., Odanacatib treatment affects trabecular and cortical bone in the femur of postmenopausal women: results of a two-year placebo-controlled trial, J. Bone Miner. Res. 30 (1) (2015) 30–38.

[10] K. Engelke, et al., Regional distribution of spine and hip QCT BMD responses after one year of once-monthly ibandronate in postmenopausal osteoporosis, Bone 46 (6) (2010) 1626–1632.

[11] H.K. Genant, et al., Improvements in hip trabecular, subcortical, and cortical density and mass in postmenopausal women with osteoporosis treated with denosumab, Bone 56 (2) (2013) 482–488.

[12] B.L. Langdahl, et al., Romosozumab (sclerostin monoclonal antibody) versus teriparatide in postmenopausal women with osteoporosis transitioning from oral bisphosphonate therapy: a randomised, open-label, phase 3 trial, Lancet 390 (10102) (2017) 1585–1594.

[13] O. Museyko, et al., QCT of the proximal femur-which parameters should be measured to discriminate hip fracture? Osteoporos. Int. 27 (3) (2016) 1137–1147.

[14] K.M. Nicks, et al., Three-dimensional structural analysis of the proximal femur in an age-stratified sample of women, Bone 55 (1) (2013) 179–188.

[15] C.E. Cann, et al., CTXA hip—an extension of classical DXA measurements using quantitative CT, PLoS One 9 (3) (2014) e91904.

[16] Y. Kang, K. Engelke, W.A. Kalender, A new accurate and precise 3-D segmentation method for skeletal structures in volumetric CT data, IEEE Trans. Med. Imaging 22 (5) (2003) 586–598.

[17] B.C. Khoo, et al., Comparison of QCT-derived and DXA-derived areal bone mineral density and T scores, Osteoporos. Int. 20 (9) (2009) 1539–1545.

[18] A.K. Amstrup, et al., Inverse correlation at the hip between areal bone mineral density measured by dual-energy X-ray absorptiometry and cortical volumetric bone mineral density measured by quantitative computed tomography, J. Clin. Densitom. 19 (2) (2016) 226–233.

[19] X. Cheng, et al., Validation of quantitative computed tomography-derived areal bone mineral density with dual energy X-ray absorptiometry in an elderly Chinese population, Chin. Med. J. 127 (8) (2014) 1445–1449.

[20] K. Engelke, et al., Clinical use of quantitative computed tomography (QCT) of the hip in the management of osteoporosis in adults: the 2015 ISCD official positions—part I, J. Clin. Densitom. 18 (3) (2015) 338–358.

[21] Y. Kang, K. Engelke, W.A. Kalender, Interactive 3D editing tools for image segmentation, Med. Image Anal. 8 (1) (2004) 35–46.

[22] Y. Kang, et al., An anatomic coordinate system of the femoral neck for highly reproducible BMD measurements using 3D QCT, Comput. Med. Imaging Graph. 29 (7) (2005) 533–541.

[23] K. Engelke, et al., A new semi-anthropometric phantom for QCT and DXA of the hip — the European Proximal Femur Phantom (EPFP). Results from the EFFECT study, 15th International Bone Densitometry Workshop, 2006 Kyoto, Japan.

[24] World Health Organization Collaborating Centre for Metabolic Bone Diseases, U.o.S, UK FRAX ® WHO Fracture Risk Assessment Tool, Available from: http://www.shef.ac.uk/FRAX/.

[25] O. Museyko, B. Gerner, K. Engelke, A new method to determine cortical bone thickness in CT images using a hybrid approach of parametric profile representation and local adaptive thresholds: accuracy results, PLoS One 12 (11) (2017) e0187097.

[26] G.M. Treece, A.H. Gee, Independent measurement of femoral cortical thickness and cortical bone density using clinical CT, Med. Image Anal. 20 (1) (2015) 249–264.

[27] G.M. Treece, et al., High resolution cortical bone thickness measurement from clinical CT data, Med. Image Anal. 14 (3) (2010) 276–290.

[28] G.M. Treece, K.E. Poole, A.H. Gee, Imaging the femoral cortex: thickness, density and mass from clinical CT, Med. Image Anal. 16 (5) (2012) 952–965.

[29] D.M. Black, et al., Proximal femoral structure and the prediction of hip fracture in men: a large prospective study using QCT, J. Bone Miner. Res. 23 (8) (2008) 1326–1333.

[30] X. Cheng, et al., Proximal femoral density and geometry measurements by quantitative computed tomography: association with hip fracture, Bone 40 (1) (2007) 169–174.

[31] F. Johannesdottir, et al., Distribution of cortical bone in the femoral neck and hip fracture: a prospective case-control analysis of 143 incident hip fractures; the AGES-REYKJAVIK Study, Bone 48 (6) (2011) 1268–1276.

[32] K.E. Poole, et al., Changing structure of the femoral neck across the adult female lifespan, J. Bone Miner. Res. 25 (3) (2010) 482–491.

[33] J. Borggrefe, et al., Association of 3D geometric measures derived from quantitative computed tomography with hip fracture risk in older men, J. Bone Miner. Res. 31 (8) (2016) 1550–1558.

[34] C.G. Miller, et al., Evaluation of quantitative computed tomography cortical hip quadrant in a clinical trial with rosiglitazone: a potential new study endpoint, J. Clin. Densitom. 19 (4) (2016) 485–491.